Permutation entropy and statistical complexity quantifier of nonstationarity effect in the vertical velocity records

Qinglei Li and Zuntao Fu

Lab for Climate and Ocean-Atmosphere Studies, Department of Atmospheric and Oceanic Sciences, School of Physics, Peking University, Beijing 100871, China

(Received 9 July 2013; published 6 January 2014)

How the nonstationarity in the atmosphere turbulent vertical velocity series affects its organization degree of multiscale structures is quantified by permutation entropy (PE) and complexity-entropy causality plane (CECP), and marked PE and CECP differences are detected between the nonstationary and stationary series. We find that the value of PE is lower in the nonstationary vertical velocity series than the stationary counterparts. Both types of series locate near the region of the higher complexity value in the CECP as chaotic systems, but the PE is smaller and the complexity degree is larger in the nonstationary series than the stationary with smaller time delays. Due to the close relationship between PE and the multiscale Shannon entropy, we show that the PE and CECP can be also taken as an indicator to quantify the different organization degrees of the multiscale structures existing between the stationary and nonstationary surface vertical velocity records.

DOI: 10.1103/PhysRevE.89.012905 PACS number(s): 05.45.Tp, 89.70.Cf, 05.40.Ca

I. INTRODUCTION

Nonstationarity is a common feature in geophysical flows, and flow in the atmospheric boundary layer is inherently nonstationary. Turbulence time series collected in the atmospheric surface layer over land may often be nonstationary. It has been found that a stationarity test shows that about 40% of the turbulent heat fluxes at Summit, Greenland are classified as nonstationary [1]. Mahrt *et al*. [2] examined the relationship of turbulence to the nonstationary wind and thermal stratification, and found that the turbulence is simultaneously generated by different nonstationary mechanisms. The related concepts of stationarity and the existence and values of integral time scales are central to the ability of analyzing micrometeorological data within the framework of Monin-Obukhov similarity theory and other classical analyses [3]. Simple and powerful methods capable of detecting the nonstationarity of a time series and studying transient dynamics would be valuable to researchers from diverse fields [4]. Therefore, the qualification of nonstationarity effect is fundamental to develop suitable models for simulation and forecasting purposes.

The nonstationarity is closely linked to the coexistence of eddies of various scales, especially the coherent structures, in the turbulent flow. In studies of atmospheric turbulence, "coherent structures" are used to denote the distinct large-scale fluctuation patterns regularly observed in a given turbulent flow [5]. It is thought that the turbulent flows are characterized by three-dimensional chaotic motions often caused by coherent eddies of different sizes and orientation [6]. It has also been pointed out that ramp features in the turbulent scalar field are associated with turbulent coherent structures, which dominate energy and mass flux in the atmospheric surface layer. Shapland *et al*. [7] demonstrated the signature of more than one ramp scale existing in structure functions of the scalar turbulence measured from above bare ground and two types of short plant canopies. The synchro-cascade pattern theory [8] has proposed that eddies of various sizes coexist and interweave with each other in each step of the cascade in the space occupied by the fluid, and their nonlinear interaction with each other strengthens or weakens their amplitudes, thereby causing strong fluctuations in amplitude with different scales. Therefore the degree of organization of complex eddy motions of various scales is really crucial to the nonstationarity of fluid turbulence. Gao *et al*. have detected nonstationarity and state transitions in a time series using recurrence time statistics and found that nonstationarity in the metastable chaotic Lorenz system is due to nonrecurrence [9,10]. In atmosphere boundary-layer turbulence, it has been found that the nonstationarity in the vertical velocity often occurs at nocturnal conditions under relatively clear skies [11], because the atmosphere boundary-layer turbulence is usually more developed during the day than the night. Also we have discovered that the probability density functions and the power spectra of the original velocity series cannot quantify the effects of the nonstationarity well [11,12].

Herein we use an approach by using quantifiers derived from information theory, permutation entropy, and statistical complexity (i) to investigate the degree of organization of complex eddy motions of various scales and (ii) to contrast the nonstationarity effect in the vertical wind velocity (w) time series collected in the atmospheric surface layer. The permutation entropy [13] and statistical complexity [14] have been used to analyze many data efficiently with low sensitivity to noise [15], by transferring the raw time series into a corresponding sequence of symbols [16–24]. The advantages of this method are its simplicity, extremely fast calculation, robustness, and invariance with respect to nonlinear monotonous transformations [13].

The rest of the paper is organized as follows. In Sec. II, we will make a short introduction of the analysis methods and the data sets used in this paper. Detailed results of permutation entropy and statistical complexity for the stationary and nonstationary vertical velocity series are provided in Sec. III. In Sec. IV, the conclusions are summarized.

II. DATA AND METHODS

A. Data

The vertical velocity records used herein were obtained from a field experiment performed by the State Key Laboratory

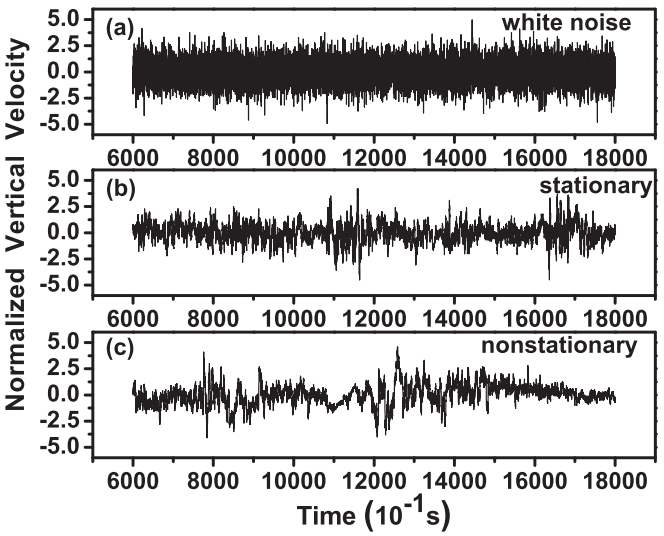

FIG. 1. Segments of the original stationary and nonstationary vertical velocity time series, with white noise for reference.

of Atmospheric Boundary-Layer Physics and Atmospheric Chemistry (LAPC), from 9 to 22 June, 1998. The underlying surface comprises paddy fields and the observation height is 4 m. The instrument used in the experiment is a SAT-211/3k three-dimensional ultrasonic anemometer, whose sampling frequency is 10 Hz and where each 40 000 sampling points are taken as one record. Typical parts of records can be found in Fig. 1, where stationary and nonstationary records show the different features; especially, there are dominant larger-scale structures in the nonstationary record. More details of the statistical characteristics of the experimental data have been shown elsewhere [11,12,25–27] and have not been repeated here for conciseness and clarity. In order to study the nonstationarity effect, we select some representative series from the data sets after the diagnosis of nonstationarity by means of the space-time index (STI) method [11,12]. The STI is a graphical method and can effectively detect dynamical nonstationarity in a time series. Detailed descriptions of the STI method are presented in Yu *et al*. [28,29]. We have selected 24 vertical velocity time series, and 12 of them are the most nonstationary among the data sets, while the other 12 are the most stationary. We show the ensemble-averaged statistical analysis results of 12 samples for each group.

B. Methods

1. Shannon entropy and permutation entropy

A nonlinear time series analysis has been used by Wesson *et al*. to quantify the organization of atmospheric turbulent eddy motion [30]. One of these nonlinear dynamic methods sensitive to distinct measures of organization of a given time series is Shannon entropy [31], which is defined as

$$S[P_i] = -\sum_i P_i \log P_i, \tag{1}$$

$P_i (i = 1,2,\ldots,M)$ is the discrete probability distribution of the given data, such as vertical wind velocity here. For further calculations, we will use the normalized Shannon entropy, $S_e = S[P_i]/\log(M)$ where M is bin number. The value of S_e is guaranteed to be between 0 and 1, and this normalization ensures that entropy differences attributed to different sampling lengths and duration are minimized [30]. Using this definition of the Shannon entropy provides a technique to give information about the order or disorder of the flow. The study by Wesson *et al*. concluded that the more intense the organization of the flow, the lower the value of the Shannon entropy [30].

Because eddies in the atmospheric turbulent motion are usually multiscaled, the Shannon entropy calculated from the original records cannot fully quantify their multiscale features [11], so we have considered the velocity increment

$$\delta v_t^\tau = v(t+\tau) - v(t), \tag{2}$$

used in structure function analysis with different time lags, $\tau = 2^h$ (delay time), to quantify the attributions from multiscale eddies with scale factor $h = 0, 1, \ldots, 9, 10$. We have calculated the P_i in Eq. (1) as the discrete probability distribution of the multiscale velocity increment δv_t^τ, and called the corresponding S_e multiscale Shannon entropy. Using multiscale Shannon entropy, different properties have been quantified between stationary and nonstationary turbulent vertical wind velocity increments. We have found that on the same scale factor the normalized Shannon entropies of stationary wind increments are all larger than those of nonstationary ones, and with the scale decreasing the normalized Shannon entropies are all dropping quickly for both stationary and nonstationary wind increments. More detailed comparative multiscale Shannon entropy results for these two types of series are presented in our previous work [11].

Similar to Shannon entropy, permutation entropy is another parameter that can quantify the organization degree of a given time series. The essence of the permutation entropy proposed by Bandt and Pompe [13] is to associate a symbolic sequence to the time series under analysis. This is done by employing a suitable partition based on ordinal patterns obtained by comparing neighboring values of the original series. This is justified if the values have a continuous distribution so that equal values are very rare. Otherwise, we can numerically break equalities by adding small random perturbations. Considering a given time series $\{x_t\}_{t=1,2,\ldots N}$, an embedding dimension $D > 1$, and a delay time τ [18], the ordinal pattern is generated by

$$(s) = (x_{s-(D-1)\tau}, x_{s-(D-2)\tau}, \ldots, x_{s-\tau}, x_s), \tag{3}$$

with $s = D\tau, D\tau+1, \ldots, N$. For each of these $(N - D\tau + 1)$ vectors, we investigate the permutations $\pi = (r_0, r_1, \ldots, r_{D-1})$ of $(0, 1, \ldots, D-1)$, defined by

$$x_{s-r_{D-1}\tau} \leqslant x_{s-r_{D-2}\tau} \leqslant \cdots \leqslant x_{s-r_1\tau} \leqslant x_{s-r_0\tau}, \tag{4}$$

and for all $D!$ possible permutations of π, we evaluate the probability distribution $P = \{p(\pi)\}$ given by

$$p(\pi) = \frac{\#\{s | s \leqslant N - D\tau + 1;\ (s) \text{ has type } \pi\}}{N - d\tau + 1}, \tag{5}$$

where the symbol # stands for the number (frequency) of occurrences of the permutation π. Thus we define the

normalized permutation entropy by

$$H_s[P] = \frac{S[p(\pi)]}{\log D!}. \quad (6)$$

Naturally, $0 \leqslant H_s[P] \leqslant 1$, where the upper bound occurs for a completely random system, i.e., a system for which all $D!$ possible permutations are equally probable. If the time series exhibits some kind of ordering dynamics $H_s[P]$ will be smaller than 1. The parameter D plays an important role in the estimation of the permutation probability distribution P, since it determines the number of accessible states [24]. In fact, the choice of D depends on the length N of the time series, in such a way that the constraint $D! \ll N$ must be satisfied in order to obtain reliable statistics. For practical purposes, Bandt and Pompe [13] recommend $D = 3, 4, \ldots, 7$, and here we have fixed $D = 6$. The parameter $\tau = 2^h$ stands for multiscale delay time [18,19] with $h = 0, 1, \ldots, 9, 10$, which is used to quantify the multiscale features in the atmospheric turbulent motions [11]. It physically corresponds to multiples of the sampling time of the given time series. Consequently, different time scales are considered by changing the embedding delay of the symbolic reconstructions [32,33].

2. *Complexity-entropy causality plane (CECP)*

López-Ruiz *et al.* [14] have introduced another statistical complexity measure able to quantify the organization degree of physical structures present in a time series, which is called the LMC complexity, named after the three authors. Given a probability distribution P as calculated in Eq. (5), this quantifier is defined by the product of the normalized entropy H_s in Eq. (6) and a suitable metric distance between P and the uniform distribution $P_e = \{1/D!\}$. We can write the LMC complexity as

$$C_{js}[P] = Q_j[P, P_e]H_s[P], \quad (7)$$

where

$$Q_j[P, P_e] = \frac{S[(P + P_e)/2] - S[P]/2 - S[P_e]/2}{Q_{\max}}, \quad (8)$$

and $Q_{\max}$ is the maximum possible value of $Q_j[P, P_e]$, obtained when one of the components of P is equal to 1 and all the others vanish, i.e.,

$$Q_{\max} = -\frac{1}{2}\left[\frac{D! + 1}{D!}\log(D! + 1) - 2\log(2D!) + \log(D!)\right]. \quad (9)$$

The quality Q_j, usually known as disequilibrium, will be different from zero if there are more likely states among the accessible ones. It is worth noting that the LMC-complexity measure C_{js} is not a trivial function of the entropy because it depends on two different probability distributions; one is associated to the system under analysis, P, and the other is uniform distribution, P_e [14]. It can quantify the existence of correlated structures [34], and provide important additional information that may not be carried only by the permutation entropy [24]. Furthermore, it was shown that for a given H_s value, there exists a range of possible C_{js} values [35]. A general procedure for obtaining the bounds $C_{js\_\min}$ and $C_{js\_\max}$ as shown in the inset graph of Fig. 4 is given by Martin *et al.* [35,36] and Rosso *et al.* [37]. Motivated by the previous discussions, Rosso *et al.* [34] proposed to employ a diagram of C_{js} versus H_s for distinguishing stochastic from chaotic behaviors. This representation space, called the complexity-entropy causality plane (CECP) [18,20,21,24,34,38,39], herein will be used to quantify different organization degrees between the stationary and nonstationary turbulent vertical wind velocity records.

To comprehensively characterize the complexity, a wide range of scales has to be considered, since the complexity is different on different scales [40]. It is clear that different time scales are taken into account by changing the embedding delays of the symbolic reconstruction [24]. The importance of selecting an appropriate embedding delay in the estimation of the permutation quantifiers has been recently confirmed for different purposes, such as identifying intrinsic time scales of delayed systems [18,23] and quantifying the degree of unpredictability of the high-dimensional chaotic fluctuations of a semiconductor laser subject to optical feedback [20]. By changing the delay times, we have found that multiscale Shannon entropy can distinguish different multiscale organization degrees between the stationary and nonstationary turbulent vertical wind velocity records [11]. Here the results deserve further investigation by using permutation entropy and statistical complexity.

III. RESULTS AND DISCUSSIONS

A. Permutation entropy and statistical complexity measure

First of all, we can see the obvious difference between the stationary and nonstationary turbulent vertical wind velocity records directly from the observational series; see Fig. 1. There are more dominant large-scale structures in the nonstationary than stationary time series; in fact, these large-scale structures will affect the results for permutation entropy analysis and statistical complexity measure.

The results of permutation entropy analysis are shown in Fig. 2. First of all, we can see that on the same scale factor, the normalized permutation entropies of stationary wind velocity are all larger than those of nonstationary ones, which indicates that there are much stronger self-correlations in

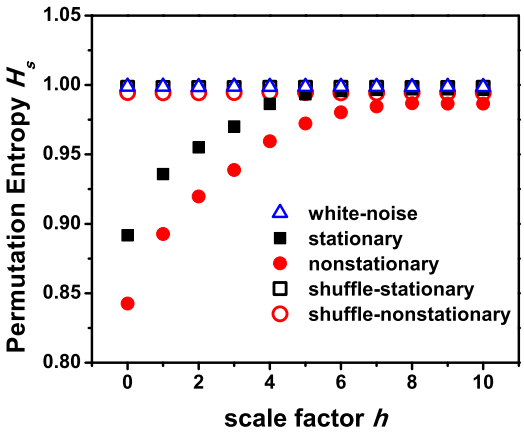

FIG. 2. (Color online) The multiscale permutation entropy for stationary and nonstationary time series, as well as the shuffled time series and white noise.

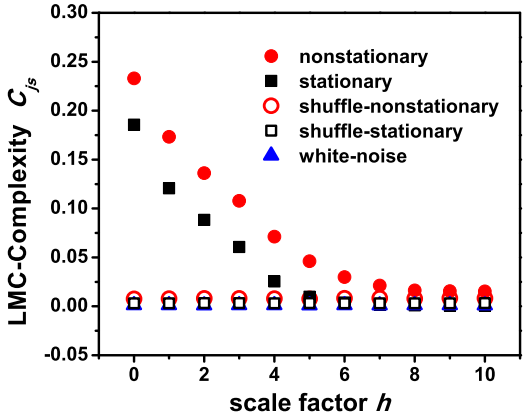

FIG. 3. (Color online) The multiscale LMC-complexity measure for stationary and nonstationary time series, as well as the shuffled time series and white noise.

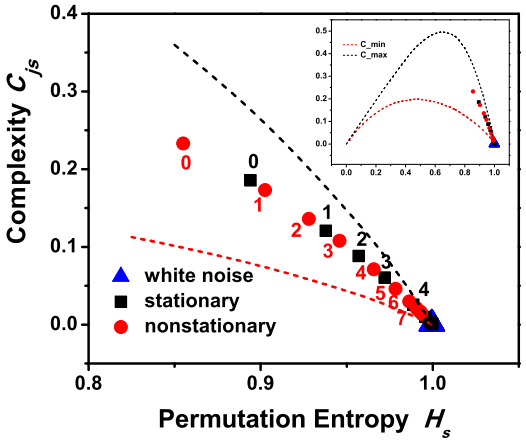

FIG. 4. (Color online) The complexity-entropy causality plane (CECP) for stationary and nonstationary vertical velocity time series. The numbers in the figure are scale factor h. The whole bounds $C_{js\_\min}$ and $C_{js\_\max}$ are shown in the inset graph.

the nonstationary than in the stationary conditions. Secondly, with the delay scale decreasing, the normalized permutation entropies are all dropping for both stationary and nonstationary records. These normalized permutation entropy features are typical of noise-free chaotic systems in the chaotic regime reported by Zunino *et al*. [19]. Thirdly, the scale at which the instability mode remains the energetic mode in the stationary wind records is much smaller than in the nonstationary flows, since the normalized permutation entropy for stationary wind records will reach its saturation level on the much smaller scale, such as $h = 5$, but for nonstationary wind velocity records, the normalized permutation entropy still does not arrive at its saturation level even when $h = 7$. At the same time, the normalized permutation entropy saturation level for the nonstationary wind velocity records is a bit lower than that for the stationary wind velocity records, which may result from the dominated non-Gaussian behaviors found in the nonstationary wind velocity records [11].

Similar features can be also found in the statistical complexity measure results, which have been shown in Fig. 3; however, the values of the statistical complexity measure on the same scale factor of stationary wind velocity are all smaller than that of nonstationary ones, which indicates there are more deterministic modes in the nonstationary records. The larger-scale structures in the nonstationary records will delay their statistical complexity measure to reach the saturation level, where the statistical complexity measure saturation level for nonstationary records is higher than that for stationary records, which may also result from the dominated non-Gaussian behaviors found in the nonstationary wind velocity records [11].

B. Complexity-entropy causality plane (CECP)

Previous studies have shown that in the CECP, all the chaotic systems have LMC complexity located near $C_{js\_\max}$. This entails that high C_{js} values are produced by structures immersed in chaotic time series [19,34]. It has also been found that $1/f^{\alpha}$ correlated stochastic processes with $1 < \alpha < 3$ are characterized by intermediate permutation entropy and intermediate statistical complexity values [34]. Here our results are consistent with these previous studies, since the turbulent flows are characterized by three-dimensional chaotic motions often caused by coherent eddies of different sizes and orientation [6]. So the vertical wind velocity time series have the higher LMC complexity values close to the $C_{js\_\max}$, regardless of whether the time series is stationary or nonstationary; see the inset graph in Fig. 4. For larger delay times, the original chaotic dynamics is undersampled, any information about the nonlinear determinism is progressively lost, and statistical behaviors of the increment series appear to be much closer to the behaviors of white noise. So the LMC complexity decreases as the delay time increases. However, the LMC complexity decreases more slowly for the nonstationary time series than the stationary counterparts, which is consistent with the analysis of PE and statistical complexity measure. We have also investigated a shuffled version of both kinds of series to verify if the localization of the vertical velocity time series in the complexity-entropy causality plane is directly related to the presence of correlations. We have obtained $H_s \approx 1$ and $C_{js} \approx 0$ for both shuffled series as white noise, which confirms that correlations inherently present in the original wind velocity records are the main source for the different locations in this plane.

IV. CONCLUSION AND DISCUSSION

In summary, we have shown that the nonstationarity in boundary-layer vertical velocity time series can be reliably characterized by estimating how the PE and LMC complexity change with the delay time increasing. For the nonstationary vertical velocity series, the permutation entropy is smaller and the LMC complexity is larger than that of stationary ones when the delay scales are smaller. In PE and CECP, the nonstationary time series reach their saturation level more slowly than the stationary counterparts as the time lags increase. The location of these quantifiers in the CECP also allows us to infer a useful organization degree of the coherent structures in boundary-layer turbulence dynamics.

Multiscale Shannon entropy has been used to quantify different organization degrees between stationary and nonstationary turbulent vertical wind velocity records [11]. What is

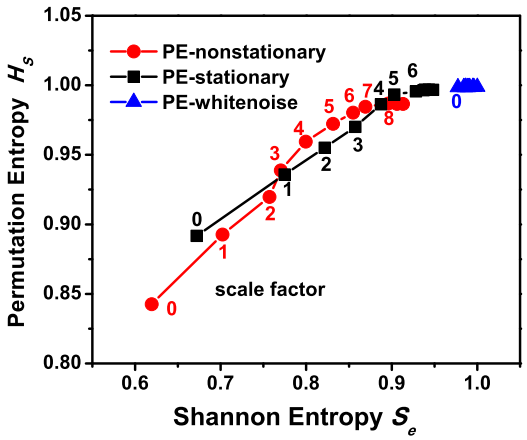

FIG. 5. (Color online) The relationship between permutation entropy and Shannon entropy for stationary and nonstationary vertical velocity time series. The numbers in the figure are scale factor h.

the relationship between PE and multiscale Shannon entropy? What is the mechanism resulting in the long-range correlations in both kinds of series? We can see there is a quite good one-to-one correspondence between PE and multiscale Shannon entropy (see Fig. 5), so the long-range correlations in both kinds of series come from the organization of eddies of different scales. Though both PE and multiscale Shannon entropy increase as the scale factor (delay time) increases, there are two differences between nonstationary and stationary time series. One difference is that the PE and multiscale Shannon entropy reach their maximums (information saturation) more slowly for nonstationary time series than the stationary counterparts. The other difference is that the PE nearly increases linearly for stationary time series, but increases nonlinearly for nonstationary time series before saturation. We have obtained $H_s \approx 1$ and $S_e \approx 1$ for both series if we shuffle them, as shown by the white noise curve in Fig. 5.

With the same data length, it is well known that the more regular the signals, the smaller entropies they have. Signals with more regularity always have smaller entropies than chaotic and random ones. It is not difficult to understand that the stationary vertical velocity has larger PE and lower LMC complexity because the atmosphere boundary-layer turbulence is usually more developed during the day. However during the night, lower PE and larger LMC complexity in nonstationary velocity could be due to the more regular, nonturbulent component of the velocity. These nonturbulent motions include wavelike motions and solitary modes, two-dimensional vortical modes, microfronts, intermittent drainage flows, and a host of more complex structures [41]. Gao *et al.* [42] have argued that the key to distinguishing chaos from noise is to identify different scale ranges where different types of motions are manifested. Here we change the delay times to study different types of motions within certain scale ranges in vertical velocity traces. For both stationary and nonstationary traces, the original chaotic dynamics is undersampled with larger delay times, any information about the nonlinear determinism is progressively lost, and statistical behaviors (such as permutation entropy and statistical complexity) of the increment series appear to be much closer to the behaviors of white noise; see Figs. 2–5. Therefore the LMC complexity decreases and the PE increases as the delay time increases.

Since multiscale Shannon entropy has been a useful tool to quantify the organization information of the coherent structures in boundary-layer turbulence dynamics, how the nonstationarity in the atmospheric turbulent vertical velocity series affects its organization degree can also be quantified by PE and CECP. Therefore the permutation entropy and statistical complexity analysis can be used to quantify the different levels of eddy organization between the stationary turbulent vertical wind records and those nonstationary ones.

ACKNOWLEDGMENTS

The authors thank the National Natural Science Foundation of China for their support through Grant No. 40975027. The valuable comments and suggestions from the anonymous reviewers are appreciated and were helpful in further improving the manuscript.

[1] N. Cullen, K. Steffen, and P. Blanken, Boundary-Layer Meteorol. **122**, 439 (2007).
[2] L. Mahrt, C. Thomas, S. Richardson, N. Seaman, D. Stauffer, and M. Zeeman, Boundary-Layer Meteorol. **147**, 179 (2013).
[3] N. Dias, M. Chamecki, A. Kan, and C. P. Okawa, Boundary-Layer Meteorol. **110**, 165 (2004).
[4] J. B. Gao, Phys. Rev. Lett. **83**, 3178 (1999).
[5] J. Wilczak, J. Atmos. Sci. **41**, 3537 (1984).
[6] B. Ganapathisubramani, N. Hutchins, W. T. Hambleton, E. K. Longmire, and I. Marusic, J. Fluid. Mech. **524**, 57 (2005).
[7] T. M. Shapland, A. J. McElrone, R. L. Snyder, and K. T. Paw U, Boundary-Layer Meteorol. **145**, 27 (2012).
[8] S. N. Zhao, X. Y. Xiong, X. H. Cui, and F. Hu, Europhys. Lett. **69**, 81 (2005).
[9] J. B. Gao, Phys. Rev. E **63**, 066202 (2001).
[10] J. B. Gao, Y. H. Cao, L. Y. Gu, J. Harris, and J. Principe, Phys. Lett. A **317**, 64 (2003).
[11] Q. L. Li and Z. T. Fu, Boundary-Layer Meteorol. **149**, 219 (2013).
[12] Z. T. Fu, Q. L. Li, N. M. Yuan, and Z. H. Yao, Commun. Nonlinear Sci. Numer. Simulat. **19**, 83 (2014).
[13] C. Bandt and B. Pompe, Phys. Rev. Lett. **88**, 174102 (2002).
[14] R. López-Ruiz, H. L. Mancini, and X. Calbet, Phys. Lett. A **209**, 321 (1995).
[15] J. Finn, J. Goettee, Z. Toroczkai, M. Anghel, and B. Wood, Chaos **13**, 444 (2003).
[16] Y. Cao, W.-w. Tung, J. B. Gao, V. A. Protopopescu, and L. M. Hively, Phys. Rev. E **70**, 046217 (2004).
[17] P. M. Saco, L. C. Carpi, A. Figliola, E. Serrano, and O. A. Rosso, Physica A **389**, 5022 (2010).

[18] L. Zunino, M. C. Soriano, I. Fischer, O. A. Rosso, and C. R. Mirasso, Phys. Rev. E **82**, 046212 (2010).
[19] L. Zunino, M. C. Soriano, and O. A. Rosso, Phys. Rev. E **86**, 046210 (2012).
[20] L. Zunino, B. M. Tabak, F. Serinaldi, M. Zanin, D. G. Pérez, and O. A. Rosso, Physica A **390**, 876 (2011).
[21] L. Zunino, M. Zanin, B. M. Tabak, D. G. Pérez, and O. A. Rosso, Physica A **389**, 1891 (2010).
[22] C. Bian, C. Qin, Q. D. Y. Ma, and Q. Shen, Phys. Rev. E **85**, 021906 (2012).
[23] M. C. Soriano, L. Zunino, O. A. Rosso, I. Fischer, and C. R. Mirasso, IEEE J. Quantum Electron. **47**, 252 (2011).
[24] H. V. Ribeiro, L. Zunino, R. S. Mendes, and E. K. Lenzi, Physica A **391**, 2421 (2012).
[25] J. Chen and F. Hu, Boundary-Layer Meteorol. **107**, 429 (2003).
[26] J. Y. Wang, Z. T. Fu, L. Zhang, and S. D. Liu, Plateau Meteorol. **24**, 5 (2005).
[27] Q. L. Li, N. Ma, and Z. T. Fu, Acta Sci. Nat. Univ. Pekin. **49**, 252 (2013).
[28] D. J. Yu, W. P. Lu, and R. G. Harrison, Phys. Lett. A **250**, 323 (1998).
[29] D. J. Yu, W. P. Lu, and R. G. Harrison, Chaos **9**, 865 (1999).
[30] K. Wesson, G. Katul, and M. Siqueira, Boundary-Layer Meteorol. **106**, 507 (2003).
[31] H. W. Wijesekera and T. M. Dillon, J. Geophys. Res. **102**, 3279 (1997).
[32] C. Bandt, Ecol. Modell. **182**, 229 (2005).
[33] J. B. Gao and H. Q. Cai, Phys. Lett. A **270**, 75 (2000).
[34] O. A. Rosso, H. A. Larrondo, M. T. Martin, A. Plastino, and M. A. Fuentes, Phys. Rev. Lett. **99**, 154102 (2007).
[35] M. T. Martin, A. Plastino, and O. A. Rosso, Physica A **369**, 439 (2006).
[36] M. T. Martin, A. Plastino, and O. A. Rosso, Phys. Lett. A **311**, 126 (2003).
[37] O. A. Rosso, M. T. Martin, and A. Plastino, Physica A **347**, 444 (2005).
[38] O. A. Rosso, L. C. Carpi, P. M. Saco, M. Gómez Ravetti, A. Plastino, and H. A. Larrondo, Physica A **391**, 42 (2012).
[39] L. Zunino, O. A. Rosso, and M. C. Soriano, IEEE J. Sel. Top. Quantum Electron. **17**, 1250 (2011).
[40] J. B. Gao, J. Hu, and W. W. Tung, Cognit. Neurodyn. **5**, 171 (2011).
[41] L. Mahrt, Annu. Rev. Fluid Mech. **46**, 23 (2014).
[42] J. B. Gao, J. Hu, W. W. Tung, and Y. H. Cao, Phys. Rev. E **74**, 066204 (2006).